Automated image analysis techniques for cardiovascular magnetic resonance imaging

Geest, R.J. van der

CHAPTER

3

Comparison between manual and automated analysis of left ventricular volume parameters from short axis MR images

This chapter was adapted from:

Comparison between manual and automated analysis of left ventricular volume parameters from short axis MR images
Rob J. van der Geest, Vincent G.M. Buller, Eric Jansen, Hildo J. Lamb, Leo H.B. Baur, Ernst E. van der Wall, Albert de Roos, Johan H.C. Reiber
Journal of Computer Assisted Tomography 1997,
Volume 21, Issue 5, Pages 756-765.

ABSTRACT

Objective: Goal of this study was to evaluate a newly developed semi-automated contour detection algorithm for the quantitative analysis cardiovascular magnetic resonance imaging.
Methods: Left ventricular function parameters derived from automatically detected endocardial and epicardial contours were compared to results derived from manually traced contours in short-axis multi-slice gradient echo MR imaging studies of ten normal volunteers and ten infarct patients.
Results: Compared to manual image analysis the semi-automated method resulted in the following systematic and random differences (auto-manual; mean ±standard deviation): end-diastolic volume: -5.5 ± 9.7 ml; end-systolic volume: -3.6 ± 6.5 ml, ejection fraction: 1.7 ± 4.1%; left ventricular mass: 7.3 ± 20.6 g. Total analysis time for a complete study was reduced from 3-4 hours for the manual analysis to less than 20 minutes using semi-automated contour detection.
Conclusion: Global left ventricular function parameters can be obtained with a high degree of accuracy and precision using the present semi-automated contour detection algorithm.

3.1 INTRODUCTION

Cardiac magnetic resonance (MR) imaging has proven to be an accurate and reproducible imaging modality for the quantitative evaluation of left ventricular function[1-8]. Gradient echo acquisitions in the short-axis orientation are particularly suitable for the assessment of left ventricular volumes and mass, as well as regional function parameters such as wall motion and wall thickening[9-11]. The assessment of these left ventricular size and function parameters, however, currently requires manual tracing of endocardial and epicardial contours in all the images to be analyzed. A typical cardiac MRI study contains 10 slices and 20 phases per cardiac cycle, i.e. 200 images in total. For most clinical applications of cardiac MRI, image analysis is limited to the end-diastolic and end-systolic time frames. However, the temporal resolution of a gradient echo MR acquisition allows the assessment of clinically valuable parameters describing the dynamics of left ventricular systolic ejection and diastolic filling, such as the peak ejection rate and filling rate[12-14]. To study these dynamic parameters, a frame-to-frame analysis needs to be carried out. While technological developments have resulted in decreased acquisition times and further improvements of image quality, the time consuming and tedious manual analysis procedure which is required to obtain the quantitative results, remains a limiting factor in the clinical use of cardiovascular MR imaging. The development of reliable automated contour detection software would be a major stimulus for the routine application of MR imaging in the evaluation of left ventricular function. To facilitate such quantitative left ventricular function analysis, we have developed the MR Analytical Software System (MASS)[15]. This software package provides manual tracing features as well as automated detection of left ventricular endocardial and epicardial contours in short-axis MR imaging studies. The use of the automated contour detection software facilitates the quantitative analysis of all phases of a multi-slice MR imaging study, thus providing assessment of left ventricular size in the end-diastolic and end-systolic phases as well as parameters describing the dynamics of left ventricular systolic ejection and diastolic filling.

The purpose of the current study was to evaluate the level of agreement between the semi-automated contour detection and manual image analysis for the assessment of global left ventricular volume parameters in gradient echo short-axis MR imaging studies using the MASS analytical software package.

3.2 METHODS

3.2.1 Study subjects

The study population consisted of 10 patients (8 men, 2 women) who had experienced myocardial infarction 3-50 weeks prior to the MR examination (average 27 weeks). The mean age of the patients was 49.6 years (range 29 - 65 years). In addition, 10 healthy volunteers (8 men, 2 women) with normal ECG and no history of cardiac malfunction were studied; mean age for this group was 30.5 years (range 21-39 years). The patient and normal studies were randomly selected from a larger database. For both sets of study subjects, the image quality was found to be acceptable for unambiguous identification of the endocardial and epicardial borders by visual inspection in the large majority (> 80%) of the images within a study.

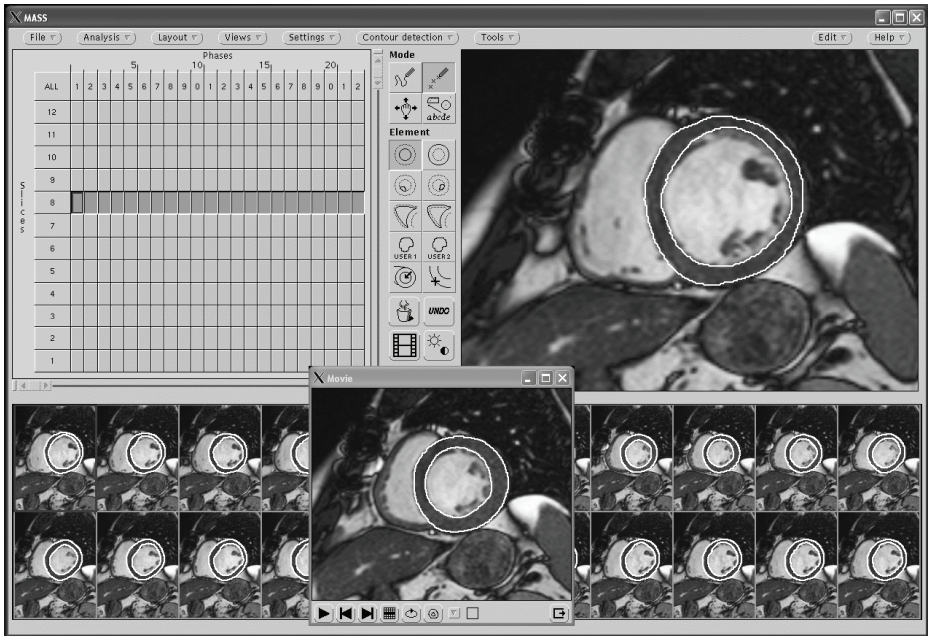

Figure 3-1. Screen layout of the MR Analytical Software System (MASS). In the upper left panel the colored bars represent all available images. The lower panel shows the time sequence of images to which the selected image belongs. The upper right panel shows the currently selected image in which contours can be edited. In a separate window a movie loop can be displayed for review of the images with the automatically detected contours.

3.2.2 Image acquisition procedure

The infarct patients were examined on a 1.5 T MR scanner (Philips Gyroscan S15, Philips Medical Systems, Best, the Netherlands) using the body coil. Spin echo scout images were obtained in the coronal and sagittal imaging planes after which the short-axis plane was determined. The short-axis plane was defined perpendicular to the left ventricular long axis from the center of the mitral annulus to the apex. In the short-axis plane 10 contiguous slices of 10 mm were obtained using standard cine-MR imaging. The echo time was 13 ms, the flip angle 50°, the repetition time equal to the average R-R interval and the field of view was 400 mm^2. The temporal resolution was 54.63 ± 1.69 ms.

The MR examinations of the normal volunteers were performed on a 1.5 T MR scanner (Philips Gyroscan ACS). Multi-slice Spin echo localizing images orientated in transversal plane were obtained. From this scan a vertical long-axis and subsequently a horizontal long-axis plane were obtained using gradient echo MR imaging. The short axis was defined from both long-axis planes. In this plane 10 slices of 8 mm with a gap of 1-2 mm were obtained using standard cine-MR imaging. The echo time was 6 ms, the flip angle 50°, the repetition time equal to the average R-R interval and the field of view was 400 mm^2. The temporal resolution was 29.16 ± 1.75 ms.

3.2.3 Analysis software

Manual and semi-automated image analysis procedures were performed using the MR Analytical Software System (MASS version 2.0) developed at our laboratory (Figure 3.1). This software package incorporates a mouse controlled graphical user-interface and runs on a SUN Sparc workstation (Mountain View, California, USA). The automated contour detection algorithm follows a model-based approach which means that existing contours are used as guiding examples for the detection of contours in neighboring phases and slices[15]. The user-interface allows manual interaction with the contour detection procedure by editing or removing incorrectly detected contours. In each contour detection iteration endocardial and epicardial contours are detected in the selected images using the manually traced or automatically detected contours as models. Manual correction can be applied at any stage of the analysis. The contour detection procedure starts with the detection of epicardial contours in the first (end-diastolic) phase of a study, followed by a frame-to-frame contour detection procedure. In the following sections the developed algorithms are described in more detail.

3.2.4 Automated detection of epicardial contours in the end-diastolic phase

To identify the location and orientation of the left ventricle in the three-dimensional data set, the Hough Transform[16] for approximately circular objects was applied to the set of images belonging to the first cardiac phase. For each of the images, the Hough Transform resulted in an image with identical dimensions as the input image, with high values near center points of objects having a radius within the specified range (7.8-39 mm). The range of radii was determined such that both endocardial and epicardial edge points would contribute to the automated determination of the ventricular center. A straight line was fit through all available Hough images to estimate the long axis of the left ventricle. This procedure resulted in an estimation of the center of the left ventricle for each slice of the imaging study.

For the detection of epicardial contours, each image was transformed to polar coordinates using the available center point. A polar edge image was computed, highlighting locations of large intensity transitions in the polar image. For each radius the edge intensity in the polar edge image was summed. Using likelihood criteria for endocardial radius and myocardial wall thickness, two out of three radii with maximum edge intensity were selected, corresponding to an endocardial and epicardial circle estimation in the original image. Next, for each radial scan line the most likely epicardial radius was derived from the five edge intensity maxima for that scan line using criteria based on the distance of that point to the circular models. If no edge point satisfied the criteria, the epicardial radius for that scan line was derived afterwards by linear interpolation. The epicardial contour detected in the polar image was transformed to image coordinates.

3.2.5 Frame-to-frame detection of epicardial contours

For the detection of epicardial contours in other phases within the cardiac cycle a frame-to-frame contour detection algorithm was developed based on matching of line profiles combined with dynamic programming[17]. A similar strategy for echocardiographic images has been described before[18]. This matching approach was developed to follow each of the different gray value transitions existing between the myocardium and anatomical regions outside the myocardium. These regions have gray values which are brighter, darker or have a gray value equal to that of the left ventricular myocardium. The gray value transition to be expected at a specific position along the circumference of the myocardium can be derived from a temporal neighboring (model) image with a known epicardial contour. The algorithm is illustrated in Figure 3-2. Given a model image (A) with known epicardial

contour, a rectangular scan matrix (mask matrix) was generated by resampling the image at equidistant points along scan lines perpendicular to the local direction of the model contour. The model scan width was optimized to be large enough to include the typical shape of the gray value profile. The actual image (B) was resampled similarly using the same model contour, but with a larger scan width. The motion of an epicardial point, assumed to be perpendicular to the local contour direction, can be estimated by matching a one-dimensional scan line of the mask image at permissible locations along the corresponding scan line of the search matrix. Using this approach a third matrix was constructed by computing the match value of mask lines at every permissible location along the corresponding search line. For this purpose the correlation coefficient was used as match value and negated such that a good match resulted in a low value in the cost matrix. In this cost matrix an optimal (minimum cost) path was generated using dynamic programming techniques. The epicardial contour for image B resulted after transformation of this path to image coordinates.

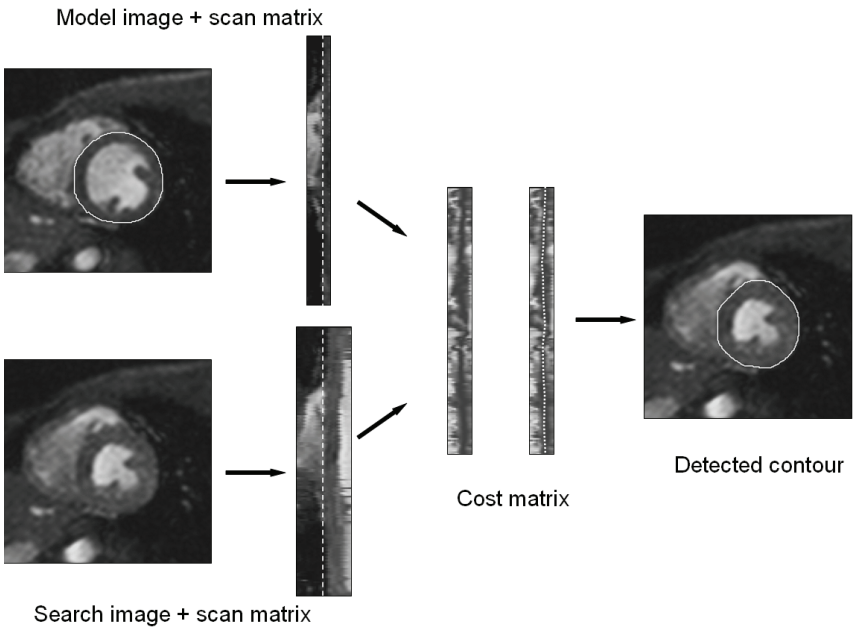

Figure 3-2. Diagram of the frame-to-frame epicardial contour detection. To detect the epicardial contour in the search image a known epicardial contour from a temporal neighboring image is used as a model. The model image is resampled perpendicularly to this epicardial contour resulting in a scan matrix. A similar scan matrix with a larger width is constructed from the search image. From both scan matrices a cost matrix is computed. The optimal path in this matrix results after transformation to the desired epicardial contour for the search image.

3.2.6 Detection of endocardial contours

The algorithm used for the detection of endocardial contours is illustrated in Figure 3-3. As a first step, an initial segmentation of the blood pool area was found using thresholding of the image within the region enclosed by the known epicardial contour. The optimal threshold was determined by generating radial scan lines emanating from the epicardial center and collecting for each scan line the gray value of the pixel with highest edge value within the epicardial contour. The mean gray value of these maximal edge pixels was designated as the optimal threshold. In a second step a smooth convex hull surrounding the blood pool area was determined resulting in an endocardial model contour. By following this approach, papillary muscles and regions caused by flow artifacts having relatively low intensity are enclosed by the contour. From this model contour a final contour was computed using minimal cost contour detection.

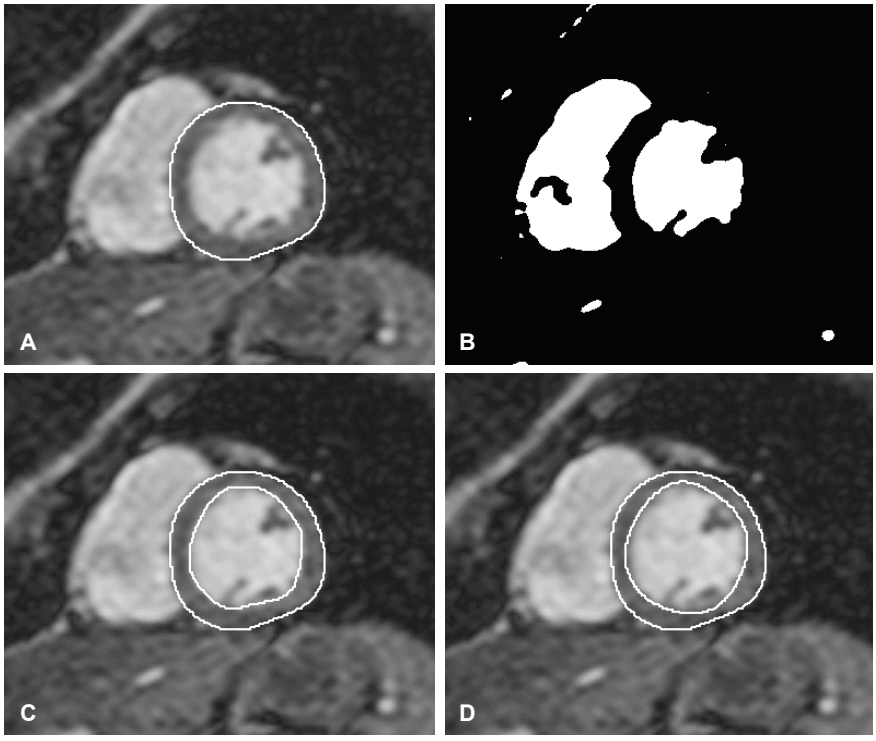

Figure 3-3. Diagram of the endocardial contour detection. The endocardial contour in an image (A) with known epicardial contour is detected by determining an optimal threshold resulting in an initial blood pool segmentation (B). A convexly shaped contour surrounding this contour is determined (C). This contour is used as a model for subsequent minimum cost contour detection resulting in the final endocardial contour (D).

3.2.7 Semi-automated analysis procedure

In this study, the following procedure was carried out. The user had to identify in which slices contours needed to be detected. In the first iteration the ventricular center was automatically detected and endocardial and epicardial contours were detected in all the selected images. After this first iteration the user was allowed to manually delete incorrect contours. In a second iteration the missing epicardial and endocardial contours were recomputed using the nearest temporal neighboring contour as the model. In case an endocardial contour was available, the region surrounding this contour was excluded from the search area of the corresponding epicardial contour. This resulted in more accurate epicardial contours in the second iteration. In case the contour detection was not entirely successful after this second iteration, the user was allowed to delete incorrect contours and manually correct at the most one single epicardial contour per slice. In the next iteration of the contour detection, the missing contours were automatically detected. In this last iteration the manually edited epicardial contour was used as the model for the detection of the missing epicardial contours in that slice. The number of manually edited epicardial contours was recorded. Manual correction to endocardial contours was not allowed at all. In the most basal slices where no complete circumference of left ventricular myocardium could be identified, the contours were traced manually.

3.2.8 Manual contour tracing

Endocardial and epicardial contours were also traced manually by an experienced observer in all the acquired phases for the slices encompassing the left ventricle. Window and level settings were standardized and kept unchanged for all studies. Papillary muscles and trabeculations were treated as being part of the blood pool[7]. In order to assess the relative overestimation of the volume of the ventricular blood pool, contours have also been traced at another occasion in the end-diastolic phase excluding the papillary muscles and trabeculations from the blood pool.

The upper slice showing at least 50% of the circumference of left ventricular myocardium was defined as the most basal slice to be included in the analysis. In this slice, the blood pool area enclosed by the myocardium and the aortic valve was included in the left ventricular volume calculations. To examine whether the contours describing the myocardial volume were traced consistently over the cardiac cycle within a single subject, the within-subject standard deviation of myocardial volume was determined for each study. A small value for this standard deviation would indicate a correct interpretation of the images over a complete cardiac

cycle. A second observer manually traced the endocardial and epicardial contours for only the end-diastolic and end-systolic phases to assess the inter-observer variabilities for this study.

3.2.9 Quantification of left ventricular mass and volume

Left ventricular volumes were measured in each phase by multiplying the contour areas by the sum of the slice thickness and slice gap. The end-diastolic volume (EDV) was obtained from the first phase after the R-wave (phase 1). End-systolic volume (ESV) was measured in the phase showing the smallest endocardial volume. Stroke volume (SV) was defined as the difference between EDV and ESV. Ejection fraction (EF) was calculated as SV divided by EDV. The left ventricular mass was determined in each phase by computing the volume of the left ventricular wall multiplied by the specific density of myocardium (1.05 g/cm^3). The peak ejection rate (PER) was defined as the maximum decrease in left ventricular volume per unit of time. The time to peak ejection rate (TPER) was defined as the time offset of the moment of PER to the R-wave. Similarly, peak filling rate (PFR) was defined as the maximum increase in left ventricular volume per unit of time. The time to peak filling rate (TPFR) was defined as the time offset of the moment of PFR from the moment of end-systole. Both PER and PFR were expressed in EDV/s.

3.3 Statistical analysis

Inter-observer variabilities expressed as mean difference ± standard deviation of paired differences were determined for left ventricular mass and volumetric function parameters. Single factor analysis of variance was used to determine the statistical significance of differences between normals and patients for each left ventricular function parameter. Linear regression analysis was used to quantify the correlation between results from semi-automated and manual image analysis. In addition, the level of agreement between manual and semi-automated image analysis was determined by computing the systematic and random differences in the calculated left ventricular volume parameters. A Student t-test was performed to determine the statistical significance of observed differences between the two measurement methods. A p-value of 0.05 was considered to indicate statistical significance.

3.4 RESULTS

3.4.1 Manual analysis

Endocardial and epicardial contours were traced manually in 2504 short-axis MR images. The total analysis time per study was 3 to 4 hours. Inter-observer variabilities for manual analysis were: EDV: 6.5 ± 16.7 ml, ESV: 4.4 ± 9.3 ml, SV: 2.0 ± 12.7 ml, EF: 0.2 ± 4.8% and left ventricular mass: 12.8 ± 23.5 g. The variation in myocardial volume over the different cardiac phases of a study resulted in a mean within-subject standard deviation of myocardial volume of 4.4%.

Table 3-1 lists the mean values and standard deviations of the quantified volumetric left ventricular function parameters for the two study groups separately. As expected the ventricular performance in the group of infarct patients was significantly reduced compared to the healthy volunteers. No difference was found in EDV (143.6 ml for patients versus 150.2 ml for normals; p=NS). ESV was significantly larger in patients (75.2 ml versus 46.3 ml; $p<0.05$) and consequently the SV (68.4 ml versus 96.4 ml; $p<0.05$) and EF (49.0% versus 69.1%; $p<0.05$) were smaller. The left ventricular mass was markedly higher in patients (177.4 versus 114.4 g; $p<0.05$). All of these measurements are based on endocardial contours which include papillary muscles and trabeculations. By manual analysis, it was found that these structures represent 6.5 ± 1.3% of the EDV. An estimation of the true EF can be made by adding this value to the measured EF.

Table 3-1. Mean values and standard deviations of ventricular dimensions and volumetric functional parameters assessed in normals and patients using manual tracing of endocardial and epicardial contours.

	Normals (n=10)		Patients (n=10)	
	Mean	SD	Mean	SD
EDV (ml)	150.2	20.3	143.6	32.0
ESV (ml)	46.3	8.4	75.2*	28.2
SV (ml)	103.9	15.6	68.4*	11.7
EF (%)	69.1	4.4	49.0*	9.2
Mass (g)	114.4	21.6	177.4*	26.1
PER (EDV/s)	4.07	0.64	2.41*	0.61
TPER (ms)	118	41	96	38
PFR (EDV/s)	4.32	0.97	2.09*	0.55
TPFR (ms)	138	22	181*	55

*: indicates statistical significant difference of values for patients compared to normals ($p<0.05$).

The parameters describing the dynamics of left ventricular ejection and filling showed a reduced PER and PFR in patients (2.41 and 2.09 EDV/s versus 4.07 and 4.32 EDV/s respectively; $p<0.05$). The timings of these events were not significantly different for TPER (96 ms versus 118 ms; p=NS) but TPFR was significantly prolonged for patients (181 ms versus 138 ms; $p<0.05$).

3.4.2 Semi-automated analysis

The semi-automated contour detection software was used to detect endocardial and epicardial contours in 2504 short-axis MR images. In the most basal slices, representing 12% of the images, the contours were traced manually. For the remaining 88% of the images the contours were detected automatically. The automated analysis time per image was in the order of 1 s per image or two minutes per study. In addition, manual correction of *epicardial* contours was necessary in 1.4% of the total number of epicardial contours (average: 2 epicardial contours per study). In 5 out of the 20 studies, the automatically detected contours did not require any manual editing. Manual editing of the automatically detected endocardial contours was not allowed in this study. The total analysis time per study for the semi-automated procedure, including careful review of the results and manual corrections, was less than 20 minutes.

Table 3-2. Systematic and random differences (auto - manual) in the assessment of left ventricular dimensions and function parameters using either semi-automated or manual image analysis.

	Normals (n=10)		Patients (n=10)		Overall (n = 20)		
	Mean	SD	Mean	SD	Mean	SD	r
EDV (ml)	-13.4*	5.7	2.4	5.7	-5.5	9.7	0.94
ESV (ml)	-5.9*	4.9	-1.4	7.1	-3.6*	6.5	0.97
SV (ml)	-7.5*	4.4	3.8	7.6	-1.9*	8.4	0.94
EF (%)	1.4	3.0	2.1	4.9	1.7*	4.1	0.95
Mass (g)	22.8*	10.2	-8.2	16.2	7.3*	20.6	0.87

EDV=end-diastolic volume; ESV=end-systolic volume; SV=stroke volume; EF=ejection fraction.

*: indicates statistical significant difference of values for patients compared to normals ($p<0.05$).

3.4.3 Comparison of left ventricular volume parameters and mass derived from manually and automatically detected contours

The agreement between semi-automated and manual analysis for the assessment of volumetric parameters is presented in Table 3-2 and further illustrated in Figure 3-4 using Bland and Altman graphs[19]. From Table 3-2 it is apparent that in the group of normal individuals the semi-automated contour detection produced slightly smaller endocardial contours which resulted in an underestimation of EDV (-13.4 ± 5.7 ml; $p<0.05$), ESV (-5.9 ± 4.9 ml; $p<0.05$) and SV (-7.5 ± 4.4 ml; $p<0.05$). This underestimation was not present in the group of patients: all differences were small and statistically not significant. An excellent agreement in EF measurement was found in both study groups; in normals a difference of 1.4 ± 3.0% (p=NS) and in patients a mean difference of 2.1 ± 4.9% (p=NS) was found. A statistically significant overestimation in myocardial mass was found in the group of healthy volunteers (22.8 ± 10.2 g; $p<0.05$). This difference is partly the result of the smaller automatically detected endocardial contours in this group. In patients the semi-automated contour detection resulted in smaller myocardial mass measurements, but this difference was found to be statistically not significant (-8.2 ± 16.2 g; p=NS).

Table 3-3. Systematic and random differences (auto - manual) of the semi-automated contour detection algorithm as compared to manually obtained results.

	Normals (n=10)		Patients (n=10)		Overall (n=20)			
	Mean	SD	Mean	SD	Mean	SD	r	r
PER (EDV/s)	0.57*	0.49	0.35*	0.29	0.46*	0.42	0.93	
TPER (ms)	6.4	25.6	10.6	33.5	8.5	29.9	0.70	
PFR (EDV/s)	-0.27	0.75	0.17	0.45	-0.05	0.66	0.86	
TPFR (ms)	-3.7	43.7	27.4	61.8	11.9	55.7	0.63	

*: indicates statistical significant difference ($p<0.05$).

3.4.4 Comparison of manually and automatically obtained left ventricular systolic ejection and diastolic filling parameters

The systematic and random differences for the measurements using semi-automated and manual image analysis are reported in Table 3-3. The semi-automated contour detection resulted in larger values for PER

(0.57 ± 0.49 EDV/s for normals and 0.35 ± 0.29 EDV/s for patients; $p<0.05$). No statistically significant differences were found in the determination of PFR (-0.27 ± 0.75 EDV/s for normals and 0.17 ± 0.45 EDV/s for patients). Manually and automatically determined values for TPER and TPFR were in excellent agreement in both study groups: the mean differences for TPER and TPFR ranged from -3.7 to + 27.4 ms (p=NS). The standard deviations of the differences ranged from 25.6 to 61.8 ms and were in the same order of magnitude as the temporal resolution

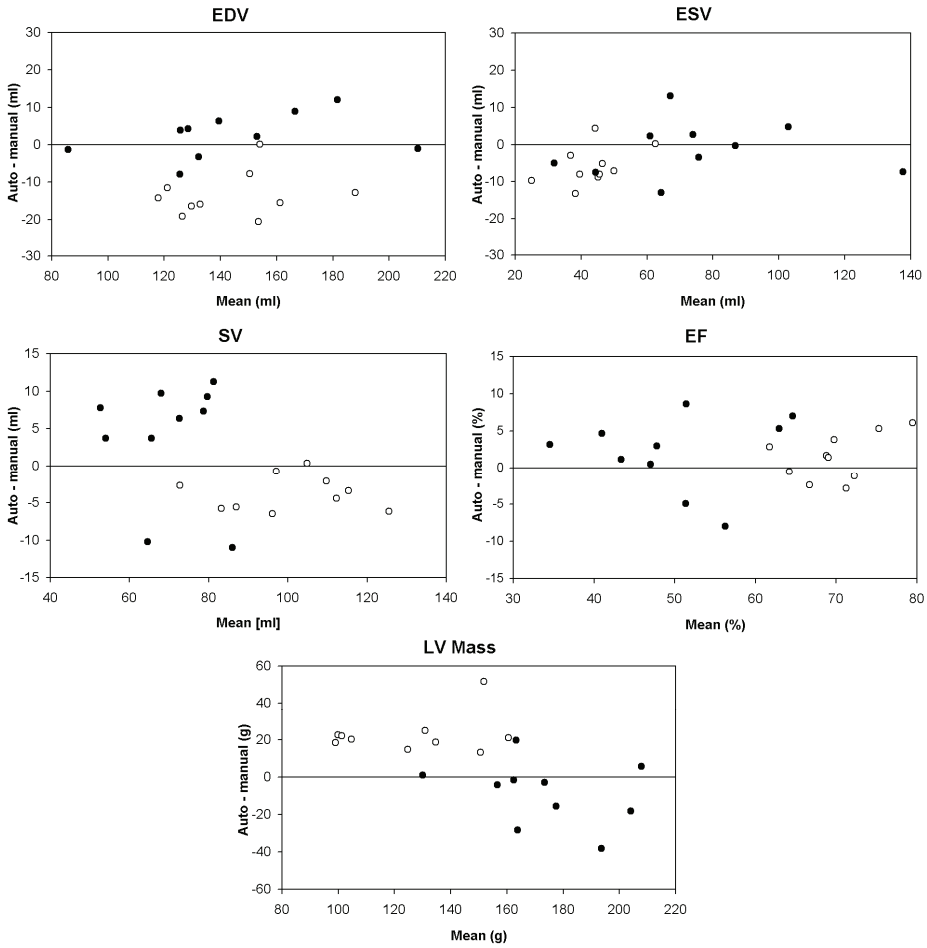

Figure 3-4. Agreement between left ventricular function parameters derived from manually traced and automatically detected contours depicted in Bland and Altman graphs. The mean value of the measurement values for automated and manual analysis is plotted along the horizontal axis; the difference between these two measurement methods is plotted along the vertical axis. Mean values of the differences and standard deviations are listed in Table 3-2. Patients are identified with a closed dot (•); volunteers are indicated by open circles (o).

3.5 DISCUSSION

Several validation studies have been performed demonstrating the accuracy and precision of left ventricular volume measurements from MR imaging acquisitions in different orientations [10-11]. The clinical value of cardiovascular MR imaging would significantly improve if the time consuming and tedious process of manual contour tracing and subsequent quantitative analysis could be automated and integrated in a dedicated software package. Towards these goals, contour detection software was developed and integrated in an analytical software package as a tool for the off-line analysis of multi-slice short-axis left ventricular MR images. As an important step towards the clinical acceptance of automated contour detection software, extensive validation is required on imaging data from normals and patients acquired on different scanners and through various imaging protocols. In the current validation study the software was utilized on MR imaging studies of normal volunteers and infarct patients acquired on two different 1.5 T MR scanners using a gradient echo pulse sequence.

3.5.1 Guidelines for tracing of endocardial contours

In the manual analysis procedure and the automated contour detection algorithm, endocardial contours were defined to describe the inner boundary of the myocardial wall[20]. With this approach the papillary muscles, either floating in the blood pool area or being connected to the myocardial wall, are considered to be no part of the myocardial muscle. This approach has two distinct advantages. First, papillary muscles and flow voids both result in dark areas within the blood pool and therefore are difficult to differentiate for an automated algorithm or a human operator. A second advantage is that the actual size of the papillary muscle is easily overestimated due to motion artifacts and partial volume effects. To be able to detect the inner wall of the myocardium according to our definition, the contours are restricted to be more or less convexly shaped. If the papillary muscles are attached to the myocardial wall or if trabeculations exist, the contour detection produces contours which cut through the attachments. A consequence of this approach is that the left ventricular blood volumes are slightly overestimated, resulting in an accurate assessment of stroke volumes, but slightly lower ejection fractions measurements. It is assumed that this disadvantage is balanced by the reduction in observer variabilities. By manual analysis it was found that the volume of the papillary muscles represents 6.5 ± 1.3% (mean ± SD) of the EDV. Consequently the true EF is 6.5% higher than the EF assessed from the endocardial contours according to our definition.

3.5.2 Guidelines for analyzing basal slices

It has been advocated that the multi-slice short-axis acquisition is ideal for left ventricular volume measurements since no geometrical assumptions are required for the analysis[21]. One of the drawbacks of this type of acquisition is that due to the relative large slice thickness that is commonly used, the most basal slices are inadequately visualized. As a result, the partial volume effect which occurs in these slices makes a correct delineation of the left ventricular myocardium often not possible unambiguously. Different observers may incorporate different guidelines to define the region belonging to the left ventricular blood pool volume and the region to be included as being left ventricular myocardium. Another factor which complicates the analysis of these basal slices in a short-axis acquisition is the fact that it is well known that the left ventricle performs not only motion in the in-plane direction, but is also characterized by a through-plane motion which is in the order of 13 mm for the normal heart[22]. This through-plane motion which extends over more than one slice makes that the shape and size of the left ventricular contours may change abruptly in the upper slices from phase to phase. Given these complications, it was decided to manually trace the contours in the endocardial and epicardial contours in the most basal slice. The circumference of the left ventricular myocardium had to extend over at least 50 percent of the circumference to be included. By comparing the variation in myocardial volume over the cardiac phases it was examined whether the contours were traced consistently. In our study the within-subject standard deviation of left ventricular myocardial volume was 4.4%, which confirms that both endocardial and epicardial contours were accurately traced in this study.

3.5.3 Automated contour detection results

The results listed in Table 3-2 should be compared to the inter-observer variabilities which were assessed in this study. The mean differences reflect a systematic over- or underestimation of one measurement technique compared to the other. Since no true gold standard is available it remains unclear which of the two techniques is more accurate. The automated contour detection algorithm resulted in smaller endocardial contours and larger epicardial contours in the group of healthy volunteers, resulting in relatively large systematic differences. Since these differences were much smaller in the studies of the infarct patients, this may have been the result of the differences in image characteristics between the two acquisitions protocols. Although two different MRI scanners were used for the patients and the normal volunteers, the main reason for the differences in image

characteristics, probably is the fact that in patient studies problems related to ECG registration and motion result in more blurring of the images. In general, systematic differences of an automated contour detection algorithm are relatively easy to solve by adjusting specific parameters in the algorithm. The standard deviations in the inter-observer analyses are relatively high when compared to the standard deviations listed in the last column of Table 3-2. This leads to the assumption that the semi-automated analysis is less hampered by random variabilities, which is especially important in follow-up studies.

No reports are known on the assessment of inter-observer variabilities for the quantification of dynamic parameters derived from multi-slice multi-phase short-axis MR studies. Table 3-3 demonstrates that the timings of the peak ejection rate and peak filling rate were determined with high accuracy and precision by the automated contour detection software. The mean differences were close to zero, while the random errors were in the same order of magnitude as the temporal resolution. The values of the dynamic parameters are in correspondence to those reported in literature[12-14].

3.5.4 Analysis time

In our experience, the manual tracing of endocardial and epicardial contours in all the phases of a multi-slice multi-phase MR study with high temporal resolution takes approximately 3 to 4 hours depending on the heart size and image quality. Using the present cardiac MR analysis software, the analysis time was reduced to less than 20 minutes on average. The actual time required for the automated contour detection for 200 images is less than 3 minutes. Manual correction to contours was performed for only two epicardial contours per study on average. The time required for reviewing the automatically detected contours and deciding whether unsatisfactory contours should be redetected in a next iteration, contributes to most of the actual analysis time. In addition, the manual tracing of contours in the most basal slice, which is still required, takes a considerable amount of time.

3.5.5 Advantages of the present contour detection algorithm

Several other studies have reported on the development and clinical evaluation of software algorithms for the semi-automated detection of left ventricular endo and/or epicardial contours in MR image data[23-25]. All these algorithms require some sort of user interaction such as manually indicating a region of interest or indication of a left ventricular center point. Although the actual computation time can be quite low in such an

approach, the required user-interactions will result in a much longer total analysis time. In our approach the required user-interaction is very much limited leading to time efficient analysis procedures. Another advantage of the present contour detection algorithm is that the epicardial contour detection is designed to be adaptive to the image characteristics and is therefore relatively insensitive to changing scan parameter settings.

3.5.6 Limitations

In this study the automated results were compared to those of one single observer. The MR examinations were performed on two different scanners using slightly different imaging protocols. Systematic differences which were found in this study may have been introduced by observer bias or by differences in the MR examination protocols. In order to further investigate the value of the present contour detection software, additional future validation studies should be performed. Repeat measurements by the same observer on separate occasions or by different observers will reveal whether the use of automated contour detection will indeed lead to a reduction in the inter- and intraobserver variabilities as compared to the manual tracing procedures. Comparison of automated contour detection results with other imaging modalities, such as stroke volume measurement by MR flow velocity mapping, may be useful to test whether systematic errors exist in the automated contour detection requiring further optimization of certain parameters in the algorithm.

3.6 Conclusion

A new analytical software package (MASS) with semi-automated contour detection has been validated on cardiovascular MR image data from patients and healthy volunteers. Quantitative left ventricular function parameters derived from the automatically detected contours were compared with results derived from manual contour tracings. This study demonstrates that volumetric left ventricular function parameters and myocardial mass can be assessed accurately in a multi-slice short-axis acquisition protocol in a time-efficient manner using the present contour detection software.

3.7 Acknowledgment

This work was financially supported in part by the Dutch Ministry of Economical Affairs and Philips Medical Systems, Best, the Netherlands.

3.8 REFERENCES

1. Florentine MS, Grosskreutz CJ, Chang W, Hartnett JA, Dunn VD, Ehrhardt JC, Fleagle SR, Collins SM, Marcus ML, Skorton DJ. Measurement of left ventricular mass in vivo using gated nuclear magnetic resonance imaging. J Am Coll Cardiol 1986; 8:107-112.
2. Sechtem U, Pflugfelder PW, Gould RG, Cassidy MM, Higgins CB. Measurement of right and left ventricular volumes in healthy individuals with cine MR imaging. Radiology 1987; 163:697-702.
3. Higgins CB, Holt W, Pflugfelder P, Sechtem U: Functional evaluation of the heart with magnetic resonance imaging. Magn Reson Med 1988; 6:121-139.
4. Buser PT, Auffermann WW, Holt WW, Wagner S, Kircher B, Wolfe C, Higgins CB. Noninvasive evaluation of global left ventricular function with use of cine nuclear magnetic resonance. J Am Coll Cardiol 1989; 11:1294-1300.
5. Semelka RC, Tomei E, Wagner S, Mayo J, Kondo C, Suzuki J, Caputo GR, Higgins CB. Normal left ventricular dimensions and function: Interstudy reproducibility of measurements with cine MR imaging. Radiology 1990; 174:763-768.
6. Semelka RC, Tomei E, Wagner S, Mayo J, Caputo G, O'Sullivan M, Parmley WW, Chatterjee K, Wolfe C, Higgins CB.. Interstudy reproducibility of dimensional and functional measurements between cine magnetic resonance studies in the morphologically abnormal LV. Am Heart J 1990;119: 1367-1373.
7. Pattynama PMT, Lamb HJ, van der Velde EA, van der Wall EE, de Roos A. Left ventricular measurements with cine and spin-echo MR imaging: a study of reproducibility with variance component analysis. Radiology 1993; 187:261-268.
8. Boxt LM, Katz J, Kolb T, Czegledy FP, Barst RJ: Direct quantitation of right and left ventricular volumes with magnetic resonance imaging in patients with primary pulmonary hypertension. J Am Coll Cardiol 1992; 19:1508-15.
9. Lotan CS, Cranney GB, Bouchard A, Bitner V, Pohost GM. The value of cine nuclear magnetic resonance imaging for assessing regional ventricular function. J Am Coll Cardiol 1983; 52:960-964.
10. van Rugge FP, van der Wall EE, Spanjersberg SJ, de Roos A, Matheijssen NAA, Zwinderman AH, van Dijkman PRM, Reiber JHC, Bruschke AVG. Magnetic resonance imaging during dobutamine stress for detection of coronary artery disease; quantitative wall motion analysis using a modification of the centerline method. Circulation 1994; 90:127-138.
11. Holman ER, Vliegen HW, van der Geest RJ, Reiber JHC, van Dijkman PRM, van der Laarse A, de Roos A, van der Wall EE. Quantitative analysis of regional left ventricular function after myocardial infarction in the pig assessed with cine magnetic resonance imaging. Magn Reson Med 1995; 34:161-169.
12. Bonow RO, Bacharach SL, Green MV, Kent KM, Rosing DR, Lipson LC, Leon MB, Epstein SE. Impaired left ventricular diastolic filling in patients with coronary artery disease: Assessment with radionuclide angiography. Circulation 1981; 2:315-323.
13. Mancini GBJ, Slutsky RA, Norris SL, Bhargava V, Ashburn WL, Higgins CB. Radionuclide analysis of peak filling rate, filling fraction and time to peak filling rate: Response to supine bicycle exercise in normal subjects and patients with coronary artery disease. Am J Cardiol 1983; 51:43-51.
14. Miller TR, Goldman KJ, Sampathkumaran KS, D.R B, Ludbrook PA, Sobel BE. Analysis of cardiac diastolic function: Application in coronary artery disease. J Nucl Med 1983; 24:2-7.
15. van der Geest RJ, Jansen E, Buller VGM, Reiber JHC. Automated detection of left ventricular epi- and endocardial contours in short-axis MR images. Comput Cardiol 1994:33-36.

16. Illingworth J, J K. A survey of the Hough transform. Computer Vision Graphics and Image Processing 1988; 44:87-116.
17. Dijkstra EW. A note on two problems in connection with graphs. Numerische Mathematik 1959; 1:269-272.
18. Bosch JG, van Burken G, Reiber JHC. Automatic frame-to-frame contour detection in echocardiograms using motion estimation. Comput Cardiol 1992: 351-354.
19. Bland JM, Altman DG. Statistical methods for assessing agreement between two methods of clinical measurement. Lancet 1986; 8:307-310.
20. Matheijssen NAA, Baur LHB, Reiber JHC, van der Velde EA, van Dijkman PRM, van der Geest RJ, de Roos A. Assessment of left ventricular volume and mass by cine-magnetic resonance imaging in patients with anterior myocardial infarction intra-observer and inter-observer variability on contour detection. Int J Cardiac Imag 1996; 12:11-19.
21. Dinsmore RE, Wismer GL, Miller SW, Thomson R, Johnston DL, Liu P, Okada RD, Saini S, Brady TJ. Magnetic resonance Imaging of the heart using imaging planes oriented to cardiac axes: experience with 100 cases. AJR 1985; 145:1177-1183.
22. Rogers WJ, Shapiro EP, Weiss JL, Buchalter MB, Rademakers FE, Weisfeldt ML, Zerhouni EA. Quantification and correction for left ventricular systolic long-axis shortening by magnetic resonance tissue tagging and slice isolation. Circulation 1991; 84:721-731.
23. Fleagle SR, Thedens DR, Stanford W, Pettigrew RI, Reichek N, Skorton DJ. Multicenter trial of automated border detection in cardiac MR imaging. J Magn Res Imag 1993; 3:409-415.
24. Fleagle SR, Thedens DR, Stanford DR, Thompson BH, Weston JM, Patel PP, Skorton DJ. Automated myocardial edge detection on MR images: accuracy in consecutive subjects. J Magn Res Imag 1993; 3:738-741.
25. Suh DY, Eisner RL, Mersereau RM, Pettigrew RI. Knowledge-based system for boundary detection of four-dimensional cardiac MR image sequences. IEEE Trans Med Imaging 1993; 12:65-72.